Published online 25 May 2012 *Nucleic Acids Research, 2012, Vol. 40, No. 15* ***7291–7302***
doi:10.1093/nar/gks452

Glucose depletion activates mmu-miR-466h-5p expression through oxidative stress and inhibition of histone deacetylation

Aliaksandr Druz[1,2], Michael Betenbaugh[2] and Joseph Shiloach[1,*]

[1]Biotechnology Core Laboratory National Institute of Diabetes and Digestive and Kidney Diseases, National Institute of Health Bldg 14A Bethesda, MD 20892 and [2]Department of Chemical and Biomolecular Engineering, Johns Hopkins University, Baltimore MD 21218, USA

Received March 10, 2012; Revised April 27, 2012; Accepted April 28, 2012

ABSTRACT

MicroRNAs (miRNAs) are involved in the regulation of multiple cellular processes. Changes of miRNA expression have been linked to the development of various diseases including cancer, but the molecular events leading to these changes at different physiological conditions are not well characterized. Here we examined the intracellular events responsible for the miR-466h-5p activation in mouse cells exposed to glucose deprivation. MiR-466h-5p is a member of the miR-297-669 cluster located in intron 10 of *Sfmbt2* gene on mouse chromosome 2 and has a pro-apoptotic role. We showed that the time-dependant activation of miR-466h-5p, miR-669c and the *Sfmbt2* gene followed the inhibition of histone deacetylation caused by glucose deprivation-induced oxidative stress. This oxidative stress causes the accumulation of reactive oxygen species (ROS) and depletion of reduced glutathione (GSH) that together inhibited histone deacetylases (HDACs) activity, reduced protein levels of HDAC2 and increased acetylation in miR-466h-5p promoter region, which led to the activation of this miRNA. Based on this study and previous work, we suggest a possible role of miR-466h-5p (and miR 297-669 cluster) in the cells during toxic metabolites accumulation. Improved characterization of the molecular events that lead to the activation of miR-466h-5p may provide a better understanding of the relation between cellular environment and miRNA activation.

INTRODUCTION

MicroRNAs (miRNAs), small non-coding single-stranded RNAs (18–25 nucleotides) have been shown to regulate gene expression in various cellular processes and functions such as cell development, differentiation, metabolism, proliferation and apoptosis (1–3). Alterations in miRNA expression profiles have been linked to cancer development and progression (1,4). Changes in miRNA expression profiles have also been explored as biomarkers for various diseases (5–7).

Although the mechanisms of miRNA-guided regulation of mRNAs expression have received considerable attention (4,8), the molecular events leading to miRNAs activation are not well known. Several studies demonstrated that miRNA expression can be regulated by transcription factors such as c-Myc, Hif-1alpha, p53 and NF-κB (8–10). Some miRNAs were shown to be regulated by the inhibition of DNA methylation and histone deacetylation (11–13), but the molecular events leading to these events under different physiological conditions are not clear.

In our previous study, we showed that the mouse miR 297-669 cluster was activated in nutrient depleted conditions (2). This cluster is located in intron 10 of the mouse *Sfmbt2* gene on Chromosome 2 and is composed of more than 40 miRNAs. All detected members of this cluster had low expression levels in CHO cells when grown in fresh media but were up-regulated in response to nutrients depletion. One member of this cluster, mmu-miR-466h-5p, was shown to have a pro-apoptotic role through targeting of several anti-apoptotic genes which led to Caspase-3/7 activation and loss of cell viability. In another study, several other members of this cluster were up-regulated when mice liver were exposed to high acetaminophen concentrations and therefore, these miRNAs were suggested as potential biomarkers for drug-induced liver injury (7). Another member of the miR 297-669 cluster, mmu-miR-669c, was shown to be associated with regulation of glutathione metabolism in the liver of aging mice (14).

In the current study, we investigated the possibility that the low expression of miR-466h-5p in cells grown in fresh media may be the result of transcriptional silencing in the promoter region of this miRNA, and that its

*To whom correspondence should be addressed. Tel: +1 301 496 9719; Fax: +1 301 451 5911; Email: yossi@nih.gov

up-regulation in nutrient-depleted conditions (2) is correlated to metabolic stress and changes in transcriptional regulation. Stress from intracellular toxicity is known to facilitate the accumulation of various reactive species, including reactive oxygen species (ROS), especially when the concentration of intracellular reduced glutathione (GSH) is low (7,15) as GSH is known to neutralize ROS and other toxic metabolites. We therefore, hypothesized that nutrient depletion leads to the accumulation of ROS and to GSH depletion that causes oxidative stress and loss of cellular detoxification capacity, triggering miR-466h-5p activation.

Glucose deprivation is a commonly investigated metabolic stress that induces signal transduction and gene expression (16,17). Indeed, glucose deprivation was shown to cause cytotoxicity and oxidative stress in human cancer cells (17–19). The lack of intracellular glucose leads to production of intracellular ROS by uncoupling glucose metabolism from the oxidative transport chain activity. Mammalian cells were shown to respond to glucose deprivation by increasing glutathione synthesis to diminish ROS generation (i.e. H_2O_2). But prolonged glucose deprivation reduced NADPH regeneration, which is necessary to keep GSH in a reduced form (17).

The accumulation of ROS can mediate the signal transduction cascade, the activation of stress kinases and substrates phosphorylation (16,19,20). Several studies have shown the reduced activity of histone deacetylases (HDACs) during oxidative stress (20–22). Histone deacetylase 2 was shown to be phosphorylated, ubiquitinated and degraded in response to oxidative stress induced by cigarette smoke (21). Reduction of HDACs activity leads to increased acetylation of histones which results in DNA uncoiling that allows the binding of transcriptional factors and increased gene expression (20,23,24).

In this study, we demonstrate that glucose deprivation leads to accumulation of ROS in a time-dependent manner that decreases HDACs activity and particularly reduces levels of HDAC2. The inhibition of HDACs activity results in the increased acetylation of miR-466h-5p promoter region and up-regulation of this miRNA. This study presents a novel approach linking the regulation of miRNA expression to the molecular events at the known physiological condition.

MATERIALS AND METHODS

Cell culture

Mouse cell lines (B/CMBA.Ov) were purchased from ATCC, Manassas, VA, USA (Cat. No. CRL-6331_FL) and grown in DMEM media supplemented with 5% non-dialyzed fetal bovine serum (Life Technologies, Gaithersburg, MD, USA). Cells were grown in 37°C, 5% CO_2 humidified incubator. Prior to any treatment, cells were counted (Cedex Roche, Indianapolis, IN, USA) and 8×10^5 cells were seeded in 100-mm tissue culture dishes and grown for 3 days in DMEM supplemented with 5% dialyzed serum (Life Technologies, Gaithersburg, MD, USA).

Cells treatment with chromatin-modifying drugs

Cells in 100 mm tissue culture dishes were treated with 1 μM or 3 μM 5-aza-2′-deoxycytidine (Sigma-Aldrich, St. Louis, MO, USA) and/or 1 mM and 3 mM 4-phenylbutyric acid (Sigma-Aldrich, St. Louis, MO, USA) (12). The drugs were dissolved in 70% ethanol at 500–1000 times their above indicated final concentration in the media. Cells were washed three times with PBS and 7 ml of fresh DMEM + 5% dialyzed serum media containing epigenetic drugs alone or in combinations were added to the plates. Two plates were used as controls: one contained the same amount of drug-free and solvent-free fresh media, and the other contained the maximum relative amount of solvent (without drugs). All measurements were performed 24 h after drug treatments.

Glucose deprivation treatment

Cells grown in 100 mm dishes in DMEM + 5% dialyzed serum media were rinsed 3 times with PBS. A quantity of 7 ml of glucose-free DMEM (Life Technologies, Gaithersburg, MD, USA) supplemented with 5% dialyzed serum were added to the plates and the samples were taken at specified time points. For control growth conditions, fresh glucose-containing DMEM + 5% dialyzed serum was added instead of glucose-free media, and samples were taken after 24 h.

Hydrogen peroxide treatments

Cells grown in 100 mm dishes in DMEM + 5% dialyzed serum media were washed 3 times with PBS. Hydrogen peroxide (H_2O_2) solutions at concentrations of 1–5 mM were prepared in DMEM + 5% dialyzed serum media from concentrated stock (8.821 M) purchased from Cell Biolabs, San Diego, CA, USA (Part No. 234102). A quanrity of 7 ml of the media containing respective amounts of H_2O_2 were then added to the plates and cells were incubated for 1, 5, 12 and 24 h.

RNA isolation and qRT–PCR analysis

Total RNA was isolated from the samples using *mir*Vana™ miRNA isolation kit, Life Technologies, Gaithersburg, MD, USA (Cat. No. AM1561). qRT–PCR analysis of the *Sfmbt2* gene and miR-466h-5p were performed in Prism 7900H Sequence Detector (Applied Biosystems, Carlbad, CA, USA) with 40 amplification cycles according to manufacturer's protocols. The *Sfmbt2* gene quantification was done using TaqMan® mRNA assay from Life Technologies (Assay ID: Mm00616783_m1) and normalized to 18S levels (Life Technologies, Assay ID: Hs99999901_s1) in the respective sample. The mmu-miR-466h-5p and miR-669c quantification was done with TaqMan® microRNA assays (Life Technologies, Assay ID: AM002516 and Assay ID:AM002646), normalized to mmu-let-7c levels (Life Technologies, Assay ID: AM00379) and analyzed as previously described (2).

Intracellular ROS detection

Intracellular ROS concentration was measured using OxiSelect™ Intracellular ROS Assay Kit with green fluorescence (Cell Biolabs, San Diego, CA, USA; Cat. No. STA-342). The cells were exposed to glucose-free media as described above for a specified time. The cells were harvested, washed with PBS, resuspended in 1 ml PBS and incubated with and without 2′,7′-dichlorodihydrofluorescin diacetate (DCFH-DA) probe (20 μM) for 45 min at 37°C with gentle vortexing in a thermal mixer. Non-fluorescent DCFH-DA probe diffuses to the cells and gets cleaved to non-fluorescent DCFH, which is rapidly oxidized to highly fluorescent 2′,7′-dichlorofluorescin (DCF) by ROS. Cells were then washed and resuspended in PBS. Flow cytometry analysis was done using ExpressPlus assay in Guava Easycyte 5HT (Millipore, Billerica, MA, USA). Cells were excited with blue laser at 488 nm and green fluorescence was determined. Dead cells and debris were gated out by forward and side scatter. The signal was first adjusted with unlabeled cells to fluorescence values below 10 (red markers in figure 4). The mean fluorescence intensity (MFI) of DCF in the labeled cells (green marker in Figure 4) corresponded to the respective levels of intracellular ROS.

Estimation of intracellular reduced GSH concentration

Cells were exposed to glucose-free media as described above. GSH levels were measured with GSH detection kit (Millipore Cat. No. APT250). The kit uses monochlorobimane (MCB) dye that fluoresces blue upon thiol binding and has a high affinity to GSH. The treated cells were collected, washed with ice-cold Wash Buffer, resuspended in Lysis buffer, incubated on ice and centrifuged. The lysates were mixed with MCB in 96-well plates and incubated at room temperature for 1.5 h. The florescence was read in the SPECTRAmax GEMINI-XS (Molecular Devices, Sunnyvale, CA, USA) spectrofluorometer using the 380-/460-nm filter set.

Measurement of HDACs activity

Following incubation in glucose-free media, the cells were collected and washed with PBS. Nuclear extracts were prepared using the NE-PER® extraction kit (Thermo Scientific, Rockford, IL, USA; Cat. No. 78833) and protein levels were quantified by the bicinchoninic acid (BCA) protein assay (Thermo Scientific, Cat. No.23227). HDACs activity was measured using a colorimetric assay kit (Enzo Life Sciences, Farmingdale, NY, USA; Cat. No. BML-AK501). The kit uses Color de Lys substrate containing deacetylated lysine side chain and is incubated with the nuclear extract. Deacetylation sensitizes the substrate and it produces a yellow chromophore upon treatment with a developer. A standard curve was first prepared using known amounts of the deacetylated standard included in the kit. The nuclear extracts (25 μg of protein) were incubated with 0.5 mM substrate in half-volume 96-well plates for 1 h at 37°C with gentle mixing. Developer solution was then added to the plate and the plate was incubated at 37°C for additional 15 min. Absorbance was analyzed with the SPECTRAmax 190 (Molecular Devices, Sunnyvale, CA, USA) plate reader at 405 nm and the values were related to known amount of deacetylated standard (Figure 3). HeLa cells nuclear extract was used as a positive control.

Western blot analysis of HDAC2

Following incubation in glucose-free media, the cells were collected and washed with PBS. Cells were lysed with RIPA buffer (Sigma, St. Louis, MO, USA; Cat. No. R0278) and protein levels were quantified by the BCA protein assay (Thermo Scientific). Protein samples (25 μg for each sample) were run on SDS–PAGE with β-actin used as the loading control. HDAC2 and β-actin were first detected with primary antibodies (Santa Cruz biotechnology, Santa Cruz, CA, USA; Cat. No. sc7899 and Abcam, Cambridge, MA, USA; Cat. No. ab6276, respectively) and then visualized using secondary antibodies conjugated with horseradish peroxidase.

QChiP assay

Chip assay was performed using the SimpleChiP™ Enzymatic Chromatin IP Kit (magnetic beads) from Cell Signaling Technology, Danvers, MA, USA (Cat. No. 9003) according to the manufacturer's protocol. The cells were exposed to glucose deprivation for indicated time, collected, cross-linked with fresh formaldehyde (MG Scientific, Pleasant Prairie, WI, USA; Cat. No. 2106-01), and treated with glycine to stop the cross-linking. At least 15 million of viable cells were used for each time point. Cells were resuspended and chromatin was fragmented by partial digestion with micrococcal nuclease. Nuclei were then broken by sonication using Ultrasonic Liquid Processor XL-2020 (Qsonica, Newtown, CT, USA) equipped with 1/16-inch probe at a setting of 2.5 and 3 sets of 15-s pulses, the lysates were centrifuged and the supernatant was collected. The chromatin concentration was determined after DNA purification from supernatant sample; its size was verified by gel electrophoresis to be between 1 and 5 nucleosomes (150–900 bp). The equivalent of ~15 μg of chromatin was diluted and incubated with either non-specific negative control normal rabbit IgG (Cell Signaling, Cat. No. 2729), positive control histone H3 rabbit mAb (pc-H3) (Cell Signaling, Cat. No. 4620) or anti-acetyl-histone H3 rabbit polyclonal Ab (Millipore, Cat. No. 17-615) overnight at 4°C with rotations. A quantity of 2% of each sample was removed before Ab incubation. Chromatin was then eluted, reverse cross-linked and DNA was purified. DNA from the 2% sample was also purified and used as control for quantitative qRT–PCR analysis. Quantitative analysis was done using SYBR detection in Prism 7900H Sequence Detector (Life Technologies) with SYBR® Green PCR Master Mix (Life Technologies, Cat. No. 4309155) according to manufacturer's protocol. Primers for qRT–PCR detection were selected within the predicted miR-466h transcription start site (25) and yielded 101 bp PCR product (forward: 5′-GTAGACTTG GTGAGTTAGAAGGCT-3′, reverse: 5′-GTGTGCAAT

CTTCTCTTTCCAAGG-3′). The fraction of DNA in the sample that was immunoprecipitated with Anti-Ac-H3 was normalized to the amount of total DNA in the sample (2% sample) and the amount of DNA was immunoprecipitated with non-specific negative control Ab (nc-Ab) as previously described (12). The pc-H3 mAb was used as an additional positive control for histone H3 detection and for qRT–PCR stringency verification. Pc-H3 precipitated DNA amounts in the miR-466h promoter areas were consistent with the amounts of total DNA in the respective samples.

RESULTS

Activation of miR-466h-5p and the *Sfmbt2* gene by histone deacetylases inhibition

The expression of several microRNAs in mammalian cells has been shown to correlate with DNA methylation and histone modifications (11–13). It was, therefore, intriguing to test the effect of the DNA-demethylating agent 5-aza-2′-deoxycytidine (Aza) and the histone deacetylases (HDACs) inhibitor, 4-phenylbutyric acid (PBA) on the activation of miR-466h-5p. Given that intronic miRNA(s) (or miRNA clusters) are known to be co-regulated with the embedding gene, the activation of *Sfmbt2* was also examined. Figure 1 shows the expression profiles of miR-466h-5p and *Sfmbt2* gene following treatment with PBA and Aza. The expression of *Sfmbt2* and miR-466h-5p was significantly increased by PBA, whereas it was not significantly affected by Aza alone or in combination with PBA (Figure 1A and B). About 1 and 3 mM of PBA in the media resulted in 3.5- and 8.1-fold induction of *Sfmbt2*, respectively, and 1.3- and 3.1-fold induction of miR-466h-5p. It is, therefore, possible that reduced levels of HDACs caused the increased expression of miR-466h-5p and *Sfmbt2* through increased histone acetylation and transcriptional activation (20,26).

Effects of glucose deprivation on miR-466h-5p expression and HDACs activity

In our previous studies, we showed that miR-466h-5p was activated when mammalian cells were exposed to nutrient-depleted conditions (2). In order to examine if altered glucose metabolism played a role in the activation of miR-466h-5p, the levels of this molecule were measured following glucose deprivation in mouse cells. Shown in Figure 2A is the time-dependent profile of miR-466h-5p during exposure to glucose-free media; this miRNA was up-regulated after 25 h of glucose-free media exposure. The 3.7- to 4.4-fold up-regulation of miR-466h-5p after 45 h of glucose-free media exposure was comparable with its activation by 3 mM of PBA (Figure 1B). Shown in Figure 2B is the time-dependant profile of another member of the miR 297-669 cluster, miR-669c, during exposure to glucose-free media. The up-regulation of miR-669c (3.8- to 4.3-fold after 45 h) and *Sfmbt2* was similar to the miR-466h-5p activation profile during glucose deprivation (Figure 2B and C).

To determine if the reduction of HDACs activity correlates with miR-466h-5p induction by glucose deprivation, HDACs activity and the protein levels of HDAC2 were measured during the glucose deprivation. Shown in Figure 3A is the time-dependant reduction of HDACs activity in cells exposed to glucose-free media. HDACs activity was reduced by >2-fold in mouse cells at and after 45 h of glucose-free media exposure compared with its activity in glucose-containing media. The protein levels of HDAC2 were also reduced following glucose deprivation (Figure 3B). This suggests that the reduction of HDACs activity during glucose deprivation can cause an increased histone acetylation and transcriptional activation, which leads to miR-466h-5p induction.

Accumulation of ROS during glucose deprivation

Glucose deprivation has been shown to induce cytotoxicity and metabolic oxidative stress as a result of increased concentrations of pro-oxidants and decreased intracellular levels of reduced GSH (16,18,19,27). It was shown previously that limited intracellular glucose caused the accumulation of reactive oxygen species (ROS) such as H_2O_2, $^{\bullet}OH$, and $O_2^{\bullet -}$ which can mediate glucose deprivation-induced oxidative stress (18). To examine the effect of glucose depletion on the mouse cells studied here, the concentrations of both ROS and reduced GSH were determined. Shown in Figure 4 are the time-dependent screens of intracellular ROS in glucose-depleted media conditions. The MFI of the DCF-labeled population of the mouse cells (shown in green) was time-dependent and directly proportional to intracellular levels of ROS. The 2.1- and 2.8-fold increase of intracellular ROS levels was observed at 45 and 50 h of glucose depletion, respectively compared with fresh media growth conditions.

Depletion of GSH in the mouse cells as a result of exposure to glucose-free media is shown in Figure 5. The time course levels of intracellular GSH levels (3.4- to 15.2-fold reduction) inversely correlated with the accumulation of the intracellular ROS (Figure 4) and the activation of miR-466h-5p (Figure 2A). These findings suggest that exposure of mouse cells to glucose-free media resulted in onset of oxidative stress shown by increased intracellular ROS generation and decreased rate of their removal likely due to GSH depletion.

Activation of miR-466h-5p by cells treatment with H_2O_2

As was shown above, glucose deprivation led to intracellular ROS accumulation (Figure 4) and to miR-466h-5p induction (Figure 2A). To verify if ROS alone can cause miR-466h-5p activation, mouse cells were treated with the pro-oxidant, H_2O_2, which is known to induce oxidative stress in mammalian cells, (15,17,22) and miR-466h-5p expression levels were determined. No significant up-regulation of miR-466h-5p was observed after 1, 5 and 12 h of cell treatment with 1–5 mM of H_2O_2 (data not shown). However, miR-466h-5p expression levels were significantly increased (1.8- to 5.3-fold) when the cells were exposed to 3 mM and higher concentrations of H_2O_2 for 24 h (Figure 6). Furthermore, activation of miR-466h-5p

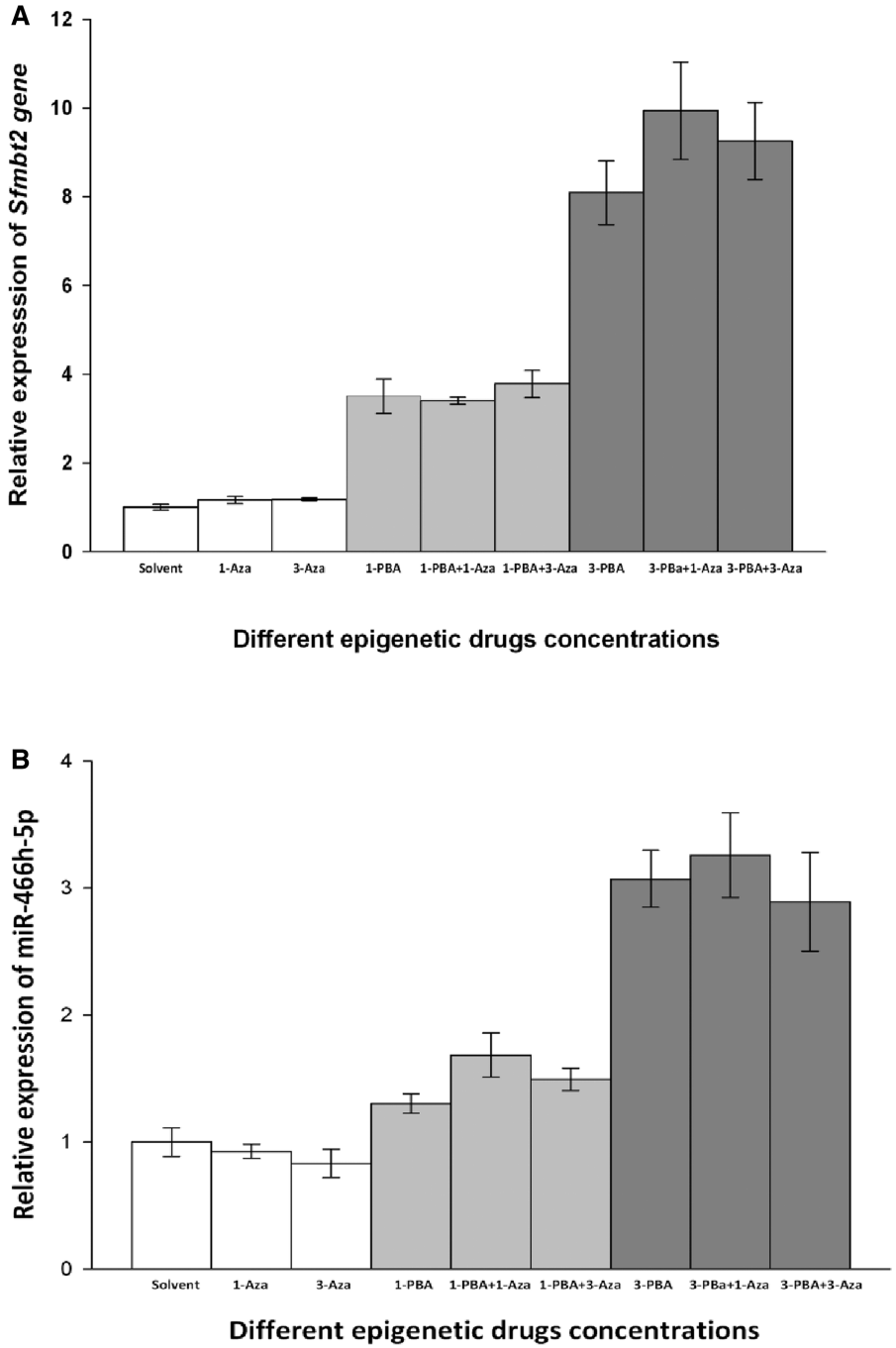

Figure 1. Expression of *Sfmbt2* gene and miR-466h-5p after 24 h of treatment with 1 mM and 3 mM of PBA and/or 1 μM and 3 μM of Aza. (**A**) Relative expression of *Sfmbt2* gene with 18S as a control for $2^{-\Delta\Delta Ct}$ analysis. (**B**) Relative expression of miR-466h-5p with let-7c as a control for $2^{-\Delta\Delta Ct}$ analysis.

by 5 mM of H_2O_2 was comparable with its activation by PBA and glucose deprivation at later times (50 h). The exogenous oxidative stress induction with 5 mM H_2O_2 for 24 h also reduced the HDACs activity to levels comparable with its activity at 45 and 50 h of glucose-free media exposure (data not shown). Hence, the induction of miR-466h-5p can be linked to decreases in HDACs activity associated with ROS during the oxidative stress.

Increased acetylation of histone 3 is associated with miR-466h-5p promoter area

As the acetylation of histone H3 is associated with transcriptional activation and gene expression (23,26,28) the acetylation of histone H3 around the predicted transcription start site of miR-466h-5p (25) was evaluated. Shown in Figure 7 is the relative amount of histone H3 acetylation associated with the miR-466h-5p promoter region as

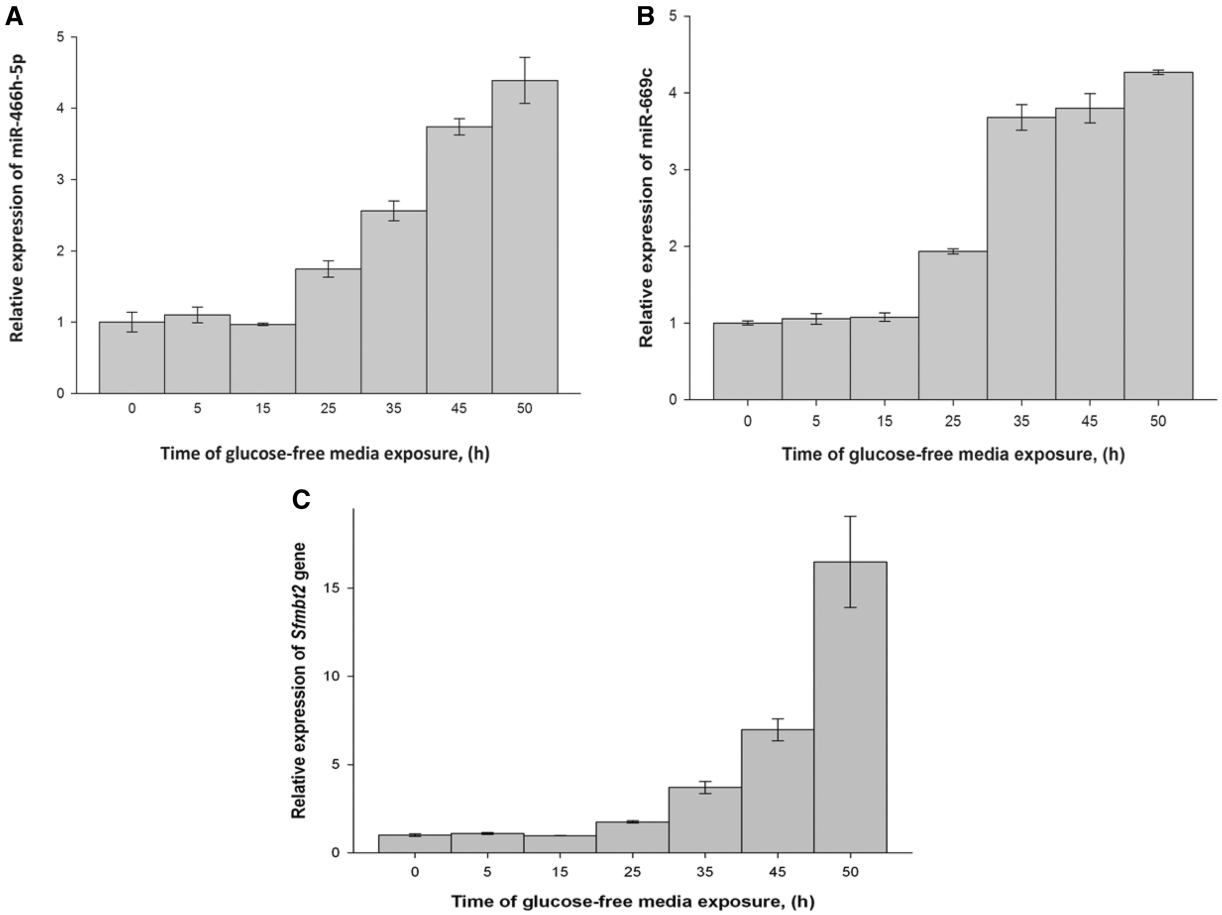

Figure 2. Time course expression of miR-466h-5p, miR-669c and *Sfmbt2* gene as a function of exposure to glucose-free media. (**A**) and (**B**) Relative expression of miR-466h-5p and miR-669c, respectively with let-7c as a control for $2^{-\Delta\Delta Ct}$ analysis. (**C**) Relative expression of *Sfmbt2* gene with 18S as a control for $2^{-\Delta\Delta Ct}$ analysis.

a function of the time the cells were exposed to glucose-free media. No significant changes in histone H3 acetylation of the miR-466h-5p promoter region was observed within the first 25 h of glucose-free media exposure. However, compared with fresh media growth conditions, acetylation of histone H3 was increased by 31, 44 and 59% after 35, 45 and 50 h exposure to glucose-free media, respectively (Figure 7). HDACs activity is known to be inhibited by oxidative stress and ROS accumulation (20–22,29). It is, therefore, possible that glucose deprivation-induced oxidative stress inhibits HDACs activity leading to increases in the acetylation of histone H3 in the miR-466h-5p promoter area and enhanced gene transcription and up-regulation of this miRNA.

DISCUSSION

miRNAs were found to be involved in regulation of multiple processes including cell differentiation, proliferation, metabolism and death (30,31), and alteration of their expression has been linked to cancer development and progression. Some studies have shown that miRNAs are frequently down-regulated or deleted in different cancers, an indication of their role as tumor suppressors (30,32,33), while other miRNAs have an oncogenic role and their inhibition can serve as a possible therapeutic approach (31,34,35). Elucidating the mechanisms controlling miRNAs' expression at different physiological and pathophysiological conditions will lead to a better understanding of the utilization of these molecules in controlling of cellular processes.

DNA modifications have been shown to have significant effects on development of human diseases (23) and several molecules that alter DNA methylation or modifications of histones are being evaluated as therapeutic agents (23). As several miRNAs were previously shown to be up-regulated by the inhibition of DNA methylation and/or inhibition of HDACs activity (11–13), we first tested which alteration affected miR-466h-5p activation. Treatments of mouse cells with 3 mM of PBA (HDACs inhibitor) resulted in up-regulation of miR-466h-5p and its embedding gene, *Sfmbt2* (3.2- and 8.1-fold, respectively). Inhibitors of HDACs (HDACi) have been explored for clinical applications as anti-cancer agents due to their ability to induce cell cycle arrest, cells differentiation and apoptosis (36–38). However, even though these agents are known to activate genes transcription, they are cytotoxic

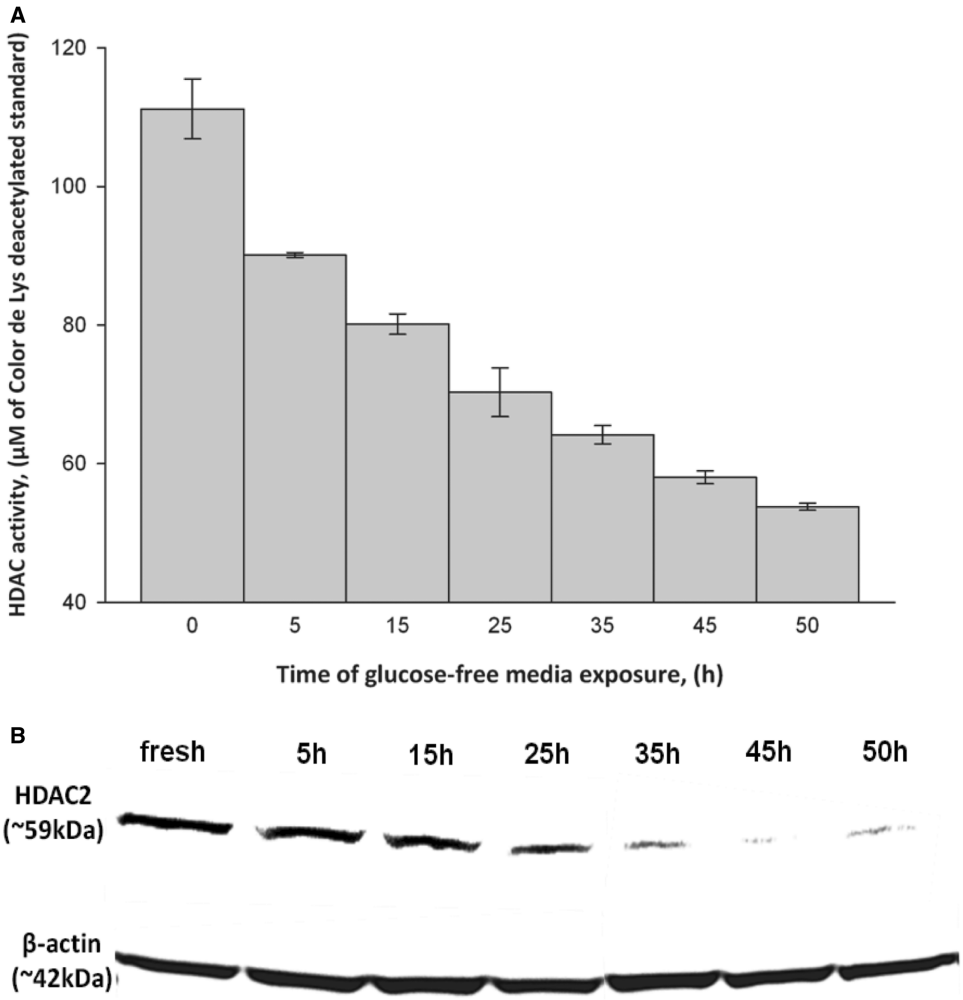

Figure 3. Time course activity of histone deacetylases and HDAC2 protein levels as a function of exposure to glucose-free media. (**A**) Histone deacetylases activity. Fluorescence values at all time points were related to the values of Color de Lys deacetylated standard. (**B**) HDAC2 proteins levels.

to the cells and there is no clear understanding of the extent of their activity (23). Understanding the role that HDACi play in miRNAs expression may enable better design of therapeutic tools for targeting specific diseases.

In the next step, we proposed the successive molecular events that caused the activation of the miR-466h-5p in mouse cells exposed to glucose deprivation. We evaluated the specific effect of glucose-free media exposure on the expression of miR-466h-5p; following 50-h exposure of miR-466h-5p and its embedding gene, *Sfmbt2*, were up-regulated 4.4-and 15-fold, respectively together with reduction of HDAC2 concentration and 2.1-fold decrease of HDACs activity. Then, we showed that the HDACs inhibition led to 59% increase of histone H3 acetylation in the miR-466h-5p promoter area, which resulted in activation of this miRNA. We also showed that exogenous induction of oxidative stress by H_2O_2 led to activation of miR-466h-5p and HDACs inhibition and verified that glucose deprivation caused the metabolic oxidative stress onset via accumulation of ROS (2.8-fold increase) and depletion of GSH (15.2-fold decrease). Shown in Figure 8 is a general outline of the suggested miR-466h-5p activation: transcriptional activation of this miRNA followed the reduction of HDAC2 activity and increased acetylation in miR-466h-5p promoter region caused by glucose deprivation-induced metabolic oxidative stress. Although we showed that glucose deprivation activated miR-466h-5p, more research needs to be conducted to determine the specific activation mechanism. It may be worthwhile to investigate the activation of specific kinases by ROS leading to post-translational modifications and the inhibition of specific HDACs involved in silencing of miR-466h-5p promoter region.

Several members of the miR 297-669 cluster, including miR-466h-5p, were also shown to be induced by acetaminophen cytotoxicity (7) which, together with our observation of miR-466h-5p induction by oxidative stress, indicates a possible role of this cluster during accumulation of toxic metabolites. The up-regulation of this miRNA cluster may be an indication of reduced cellular detoxification capacity and may be explored as biomarker for drugs-induced cellular injuries (7). As miR-466h-5p

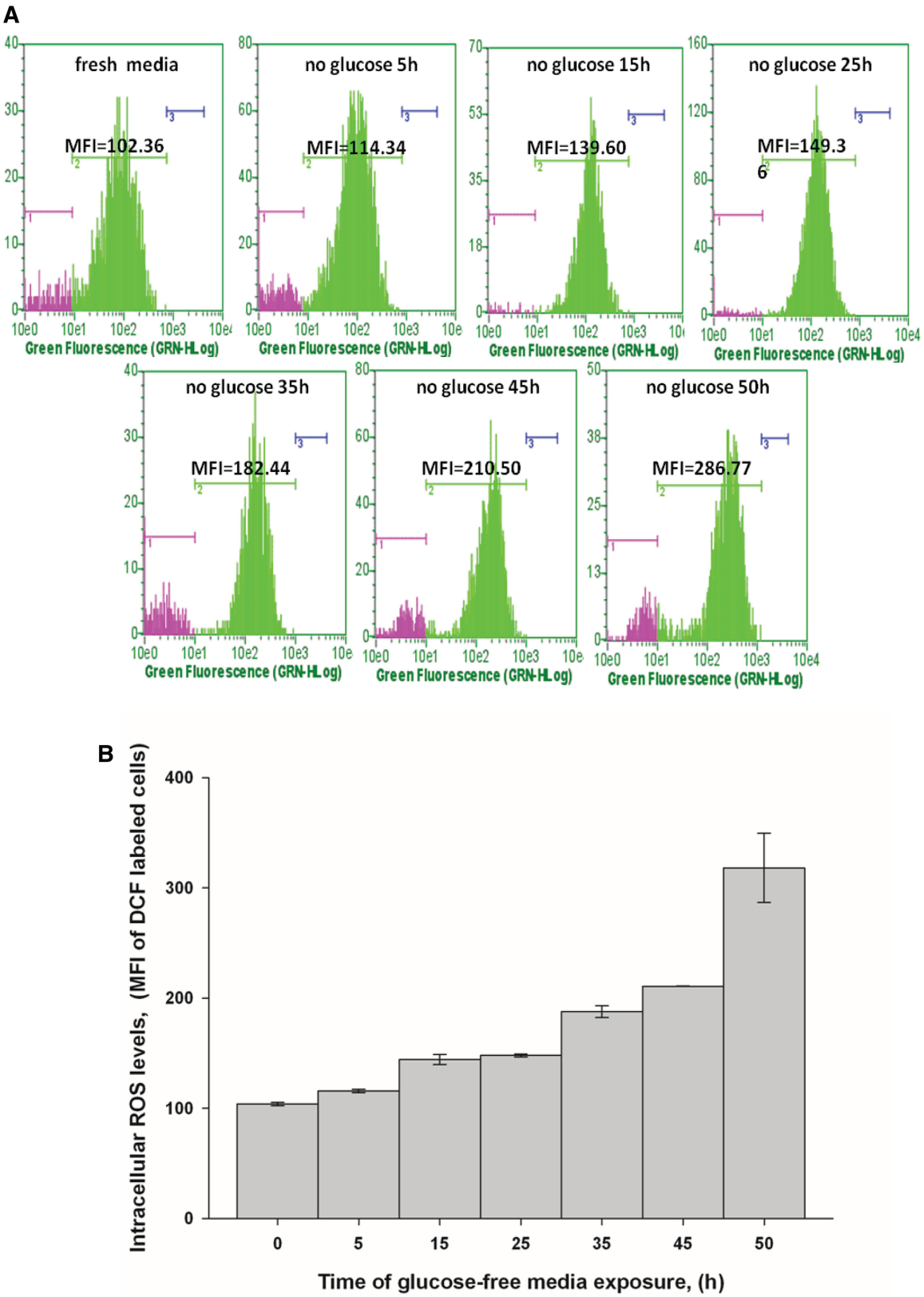

Figure 4. Intracellular levels of ROS as a function of exposure to glucose-free media. (**A**) Fluorescence-activated cell sorter (FACS) image of fluorescence intensity distribution of DCF-labeled cells (green marker) exposed to glucose-free media for indicated time points. Mean fluorescent intensity value (MFI) is proportional to intracellular levels of ROS. (**B**) Accumulation of ROS with time of glucose-free media exposure.

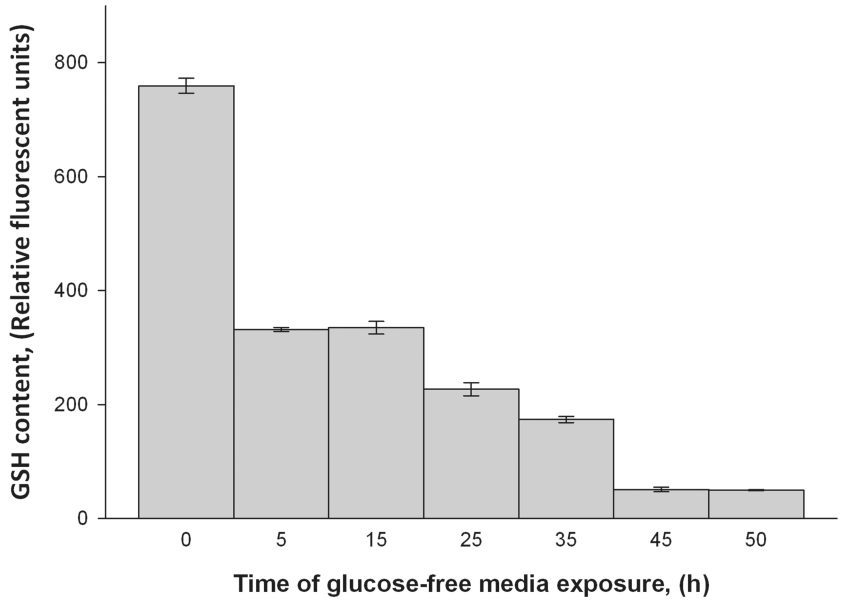

Figure 5. Time course levels of GSH levels as a function of exposure to glucose-free media.

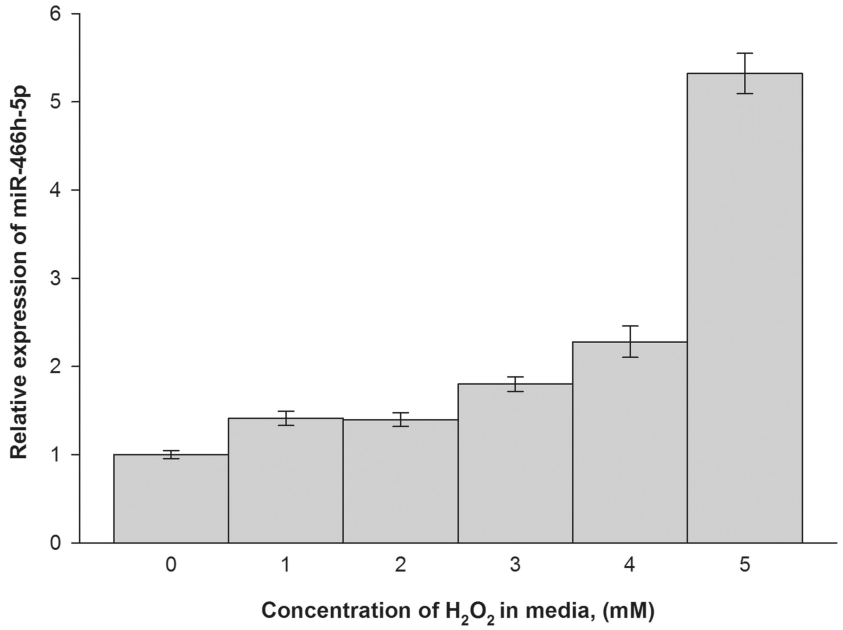

Figure 6. Relative expression of miR-466h-5p after treatment with H_2O_2 for 24 h.

was previously shown to have a pro-apoptotic role by down-regulating several anti-apoptotic genes including *bcl2l2*, *birc6*, *dad1*, *smo* and *stat5a*, (2) and given the fact that clustered miRNA are usually transcribed together as polycistronic transcripts to regulate genes with similar functions (31,39), the miR 297-669 cluster may be induced in mammalian cells exposed to cytotoxic conditions. This induction could be inhibited during oncogenic transformation as cancer development is known to result from the loss of oxidative stress defense mechanisms (27,40,41). As the predicted transcription start sites for all members of the miR 297-669 cluster is located directly upstream of *Sfmbt2* gene (25), all members of this miRNA cluster may be co-transcribed in response to cytotoxic stimuli; the up-regulation of both miR-466h-5p and miR-669c by glucose deprivation (Figure 2A and B) supported this assumption. The *Sfmbt2* gene belongs to the Scm-family of Polycomb transcriptional repressor genes and has four mbt domains known to have tumor suppressor activity (42,43). This gene has been implicated in development of brain tumor and neurological disorders (42,44). Although the inhibition of some Polycomb group

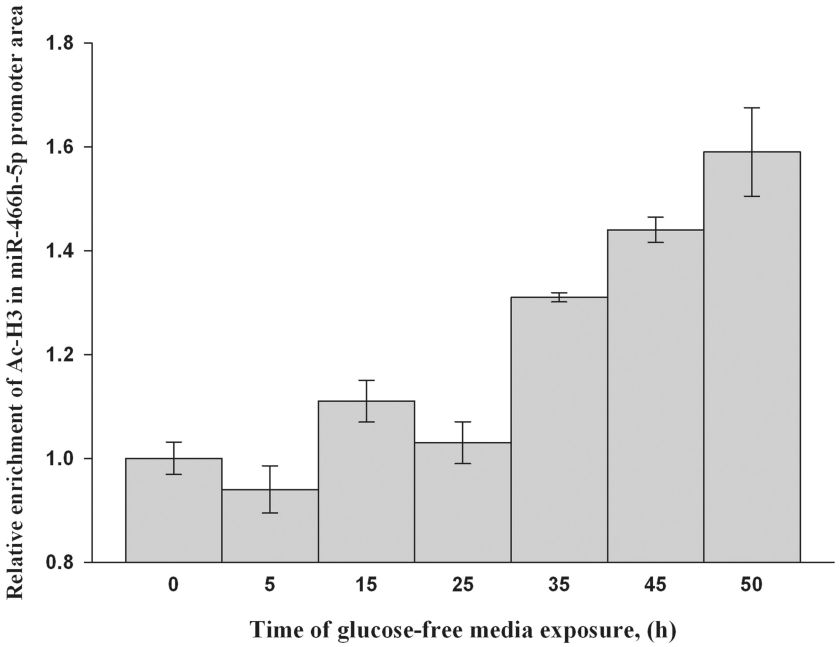

Figure 7. Acetylation of histone H3 in miR-466h-5p promoter area as a function of time of exposure to glucose-free media. The amounts of DNA bound to Ac-H3 were related to its amount in fresh media grown cells.

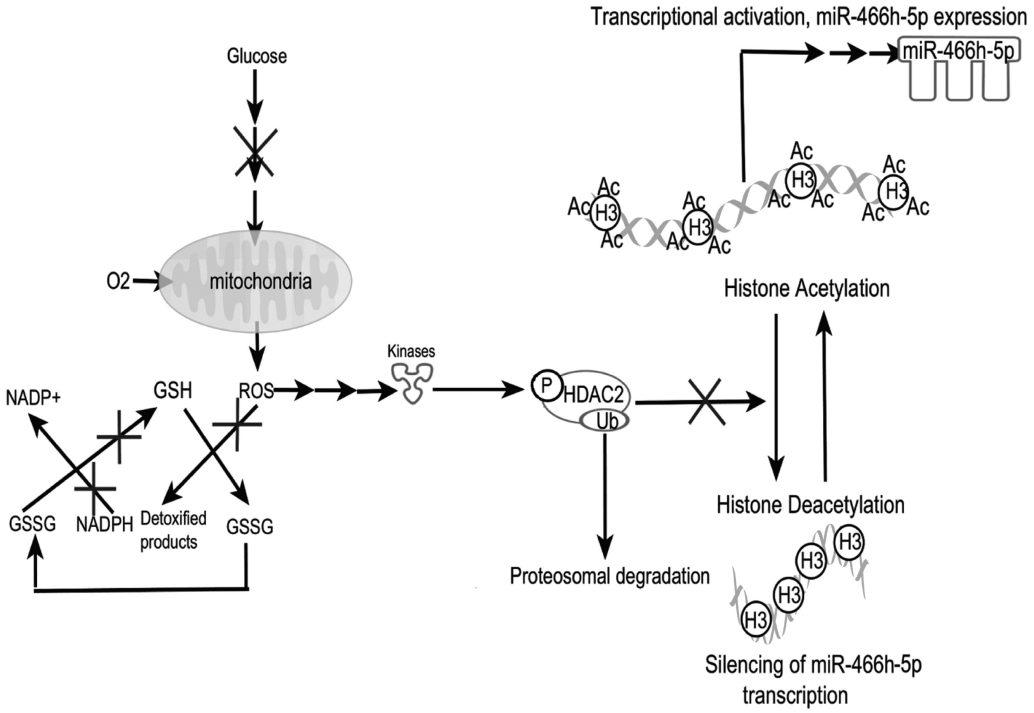

Figure 8. Suggested mechanism of miR-466h-5p activation. Glucose depletion leads to accumulation of ROS and inhibition of HDACs activity that increases histone H3 acetylation and activates miR-466h-5p (figure was created using 'pathway designer' tool in IPA Ingenuity Software).

proteins was shown to be associated with the inhibition of HDACs activity (45), the *Sfmbt2* gene was previously shown to be activated by valproate, the mood stabilizer known to increase acetylation of histone H3 in mouse brain cells (43,46), and to selectively reduce the levels of HDAC2 (47). Further studies need to be conducted to verify the activation of the other miR 297-669 cluster members and to elucidate the role of *Sfmbt2* gene in this activation.

Our study is a novel approach to link the miRNA activation to a known physiological condition and it shows the importance of understanding the mechanisms of

miRNAs activation. Together with previous reports, it suggests a potential role of miR 297-669 cluster and its embedding gene, *Sfmbt2*, in development of various diseases (2,7,42,44).

ACKNOWLEDGEMENTS

The authors would like to thank Dr. J. Hanover for critical review of the manuscript and Mrs. D. Livnat for critical editorial assistance.

FUNDING

Funding for open access charge: Intramural program of the National Institute of Diabetes and Digestive and Kidney Diseases, National Institutes of Health.

Conflict of interest statement. None declared.

REFERENCES

1. Jovanovic,M. and Hengartner,M.O. (2006) miRNAs and apoptosis: RNAs to die for. *Oncogene*, **25**, 6176–6187.
2. Druz,A., Chu,C., Majors,B., Santuary,R., Betenbaugh,M. and Shiloach,J. (2011) A novel microRNA mmu-miR-466h affects apoptosis regulation in mammalian cells. *Biotechnol. Bioeng.*, **108**, 1651–1661.
3. Mendell,J.T. (2005) MicroRNAs: critical regulators of development, cellular physiology and malignancy. *Cell Cycle*, **4**, 1179–1184.
4. Lynam-Lennon,N., Maher,S.G. and Reynolds,J.V. (2009) The roles of microRNA in cancer and apoptosis. *Biol. Rev. Camb. Philos. Soc.*, **84**, 55–71.
5. Fichtlscherer,S., Zeiher,A.M. and Dimmeler,S. (2011) Circulating microRNAs: biomarkers or mediators of cardiovascular diseases? *Arterioscler. Thromb. Vasc. Biol.*, **31**, 2383–2390.
6. Keller,A., Backes,C., Leidinger,P., Kefer,N., Boisguerin,V., Barbacioru,C., Vogel,B., Matzas,M., Huwer,H., Katus,H.A. *et al.* (2011) Next-generation sequencing identifies novel microRNAs in peripheral blood of lung cancer patients. *Mol. Biosyst.*, **7**, 3187–3199.
7. Wang,K., Zhang,S., Marzolf,B., Troisch,P., Brightman,A., Hu,Z., Hood,L.E. and Galas,D.J. (2009) Circulating microRNAs, potential biomarkers for drug-induced liver injury. *Proc. Natl Acad. Sci. USA*, **106**, 4402–4407.
8. Chang,T.C., Yu,D., Lee,Y.S., Wentzel,E.A., Arking,D.E., West,K.M., Dang,C.V., Thomas-Tikhonenko,A. and Mendell,J.T. (2008) Widespread microRNA repression by Myc contributes to tumorigenesis. *Nat. Genet.*, **40**, 43–50.
9. O'Donnell,K.A., Wentzel,E.A., Zeller,K.I., Dang,C.V. and Mendell,J.T. (2005) c-Myc-regulated microRNAs modulate E2F1 expression. *Nature*, **435**, 839–843.
10. Sun,W., Julie Li,Y.S., Huang,H.D., Shyy,J.Y. and Chien,S. (2010) microRNA: a master regulator of cellular processes for bioengineering systems. *Annu. Rev. Biomed. Eng.*, **12**, 1–27.
11. Bandres,E., Agirre,X., Bitarte,N., Ramirez,N., Zarate,R., Roman-Gomez,J., Prosper,F. and Garcia-Foncillas,J. (2009) Epigenetic regulation of microRNA expression in colorectal cancer. *Int. J. Cancer*, **125**, 2737–2743.
12. Saito,Y., Liang,G., Egger,G., Friedman,J.M., Chuang,J.C., Coetzee,G.A. and Jones,P.A. (2006) Specific activation of microRNA-127 with downregulation of the proto-oncogene BCL6 by chromatin-modifying drugs in human cancer cells. *Cancer Cell*, **9**, 435–443.
13. Scott,G.K., Mattie,M.D., Berger,C.E., Benz,S.C. and Benz,C.C. (2006) Rapid alteration of microRNA levels by histone deacetylase inhibition. *Cancer Res.*, **66**, 1277–1281.
14. Maes,O.C., An,J., Sarojini,H. and Wang,E. (2008) Murine microRNAs implicated in liver functions and aging process. *Mech. Ageing Dev.*, **129**, 534–541.
15. Kim,S.J., Jung,H.J. and Lim,C.J. (2011) Disruption of redox homeostasis and induction of apoptosis by suppression of glutathione synthetase expression in a mammalian cell line. *Free Radic. Res.*, **45**, 1040–1051.
16. Blackburn,R.V., Spitz,D.R., Liu,X., Galoforo,S.S., Sim,J.E., Ridnour,L.A., Chen,J.C., Davis,B.H., Corry,P.M. and Lee,Y.J. (1999) Metabolic oxidative stress activates signal transduction and gene expression during glucose deprivation in human tumor cells. *Free Radic. Biol. Med.*, **26**, 419–430.
17. Spitz,D.R., Sim,J.E., Ridnour,L.A., Galoforo,S.S. and Lee,Y.J. (2000) Glucose deprivation-induced oxidative stress in human tumor cells. A fundamental defect in metabolism? *Ann. NY Acad. Sci.*, **899**, 349–362.
18. Ahmad,I.M., Aykin-Burns,N., Sim,J.E., Walsh,S.A., Higashikubo,R., Buettner,G.R., Venkataraman,S., Mackey,M.A., Flanagan,S.W., Oberley,L.W. *et al.* (2005) Mitochondrial O_2*- and H_2O_2 mediate glucose deprivation-induced stress in human cancer cells. *J. Biol. Chem.*, **280**, 4254–4263.
19. Lee,Y.J., Galoforo,S.S., Berns,C.M., Chen,J.C., Davis,B.H., Sim,J.E., Corry,P.M. and Spitz,D.R. (1998) Glucose deprivation-induced cytotoxicity and alterations in mitogen-activated protein kinase activation are mediated by oxidative stress in multidrug-resistant human breast carcinoma cells. *J. Biol. Chem.*, **273**, 5294–5299.
20. Rahman,I., Marwick,J. and Kirkham,P. (2004) Redox modulation of chromatin remodeling: impact on histone acetylation and deacetylation, NF-kappaB and pro-inflammatory gene expression. *Biochem. Pharmacol.*, **68**, 1255–1267.
21. Adenuga,D., Yao,H., March,T.H., Seagrave,J. and Rahman,I. (2009) Histone deacetylase 2 is phosphorylated, ubiquitinated, and degraded by cigarette smoke. *Am. J. Respir. Cell Mol. Biol.*, **40**, 464–473.
22. Ito,K., Lim,S., Caramori,G., Chung,K.F., Barnes,P.J. and Adcock,I.M. (2001) Cigarette smoking reduces histone deacetylase 2 expression, enhances cytokine expression, and inhibits glucocorticoid actions in alveolar macrophages. *FASEB J.*, **15**, 1110–1112.
23. Egger,G., Liang,G., Aparicio,A. and Jones,P.A. (2004) Epigenetics in human disease and prospects for epigenetic therapy. *Nature*, **429**, 457–463.
24. Lu,Q., Qiu,X., Hu,N., Wen,H., Su,Y. and Richardson,B.C. (2006) Epigenetics, disease, and therapeutic interventions. *Ageing Res. Rev.*, **5**, 449–467.
25. Marson,A., Levine,S.S., Cole,M.F., Frampton,G.M., Brambrink,T., Johnstone,S., Guenther,M.G., Johnston,W.K., Wernig,M., Newman,J. *et al.* (2008) Connecting microRNA genes to the core transcriptional regulatory circuitry of embryonic stem cells. *Cell*, **134**, 521–533.
26. Clayton,A.L., Hazzalin,C.A. and Mahadevan,L.C. (2006) Enhanced histone acetylation and transcription: a dynamic perspective. *Mol. Cell*, **23**, 289–296.
27. Davis,W. Jr, Ronai,Z. and Tew,K.D. (2001) Cellular thiols and reactive oxygen species in drug-induced apoptosis. *J. Pharmacol. Exp. Ther.*, **296**, 1–6.
28. Zhao,Y., Lu,J., Sun,H., Chen,X., Huang,W., Tao,D. and Huang,B. (2005) Histone acetylation regulates both transcription initiation and elongation of hsp22 gene in Drosophila. *Biochem. Biophys. Res. Commun.*, **326**, 811–816.
29. Yang,S.R., Chida,A.S., Bauter,M.R., Shafiq,N., Seweryniak,K., Maggirwar,S.B., Kilty,I. and Rahman,I. (2006) Cigarette smoke induces proinflammatory cytokine release by activation of NF-kappaB and posttranslational modifications of histone deacetylase in macrophages. *Am. J. Physiol. Lung Cell Mol. Physiol.*, **291**, L46–L57.
30. Calin,G.A., Dumitru,C.D., Shimizu,M., Bichi,R., Zupo,S., Noch,E., Aldler,H., Rattan,S., Keating,M., Rai,K. *et al.* (2002) Frequent deletions and down-regulation of micro- RNA genes miR15 and miR16 at 13q14 in chronic lymphocytic leukemia. *Proc. Natl Acad. Sci. USA*, **99**, 15524–15529.
31. Hayashita,Y., Osada,H., Tatematsu,Y., Yamada,H., Yanagisawa,K., Tomida,S., Yatabe,Y., Kawahara,K., Sekido,Y.

and Takahashi,T. (2005) A polycistronic microRNA cluster, miR-17-92, is overexpressed in human lung cancers and enhances cell proliferation. *Cancer Res.*, **65**, 9628–9632.
32. Michael,M.Z., O' Connor,S.M., van Holst Pellekaan,N.G., Young,G.P. and James,R.J. (2003) Reduced accumulation of specific microRNAs in colorectal neoplasia. *Mol. Cancer Res.*, **1**, 882–891.
33. Takamizawa,J., Konishi,H., Yanagisawa,K., Tomida,S., Osada,H., Endoh,H., Harano,T., Yatabe,Y., Nagino,M., Nimura,Y. *et al.* (2004) Reduced expression of the let-7 microRNAs in human lung cancers in association with shortened postoperative survival. *Cancer Res.*, **64**, 3753–3756.
34. Chan,J.A., Krichevsky,A.M. and Kosik,K.S. (2005) MicroRNA-21 is an antiapoptotic factor in human glioblastoma cells. *Cancer Res.*, **65**, 6029–6033.
35. Voorhoeve,P.M., le Sage,C., Schrier,M., Gillis,A.J., Stoop,H., Nagel,R., Liu,Y.P., van Duijse,J., Drost,J., Griekspoor,A. *et al.* (2006) A genetic screen implicates miRNA-372 and miRNA-373 as oncogenes in testicular germ cell tumors. *Cell*, **124**, 1169–1181.
36. Dokmanovic,M. and Marks,P.A. (2005) Prospects: histone deacetylase inhibitors. *J. Cell Biochem.*, **96**, 293–304.
37. Drummond,D.C., Noble,C.O., Kirpotin,D.B., Guo,Z., Scott,G.K. and Benz,C.C. (2005) Clinical development of histone deacetylase inhibitors as anticancer agents. *Annu. Rev. Pharmacol. Toxicol.*, **45**, 495–528.
38. Rosato,R.R. and Grant,S. (2005) Histone deacetylase inhibitors: insights into mechanisms of lethality. *Expert Opin. Ther. Targets*, **9**, 809–824.
39. Liang,R., Bates,D.J. and Wang,E. (2009) Epigenetic control of microRNA Expression and aging. *Curr. Genomics*, **10**, 184–193.
40. Kryston,T.B., Georgiev,A.B., Pissis,P. and Georgakilas,A.G. (2011) Role of oxidative stress and DNA damage in human carcinogenesis. *Mutat. Res.*, **711**, 193–201.
41. Zhang,H., Kong,X., Kang,J., Su,J., Li,Y., Zhong,J. and Sun,L. (2009) Oxidative stress induces parallel autophagy and mitochondria dysfunction in human glioma U251 cells. *Toxicol. Sci.*, **110**, 376–388.
42. Bonasio,R., Lecona,E. and Reinberg,D. (2010) MBT domain proteins in development and disease. *Semin. Cell Dev. Biol.*, **21**, 221–230.
43. Chetcuti,A., Adams,L.J., Mitchell,P.B. and Schofield,P.R. (2006) Altered gene expression in mice treated with the mood stabilizer sodium valproate. *Int. J. Neuropsychopharmacol.*, **9**, 267–276.
44. Becanovic,K., Pouladi,M.A., Lim,R.S., Kuhn,A., Pavlidis,P., Luthi-Carter,R., Hayden,M.R. and Leavitt,B.R. (2010) Transcriptional changes in Huntington disease identified using genome-wide expression profiling and cross-platform analysis. *Hum. Mol. Genet.*, **19**, 1438–1452.
45. Bommi,P.V., Dimri,M., Sahasrabuddhe,A.A., Khandekar,J. and Dimri,G.P. (2010) The polycomb group protein BMI1 is a transcriptional target of HDAC inhibitors. *Cell Cycle*, **9**, 2663–2673.
46. Correa,F., Mallard,C., Nilsson,M. and Sandberg,M. (2011) Activated microglia decrease histone acetylation and Nrf2-inducible anti-oxidant defence in astrocytes: restoring effects of inhibitors of HDACs, p38 MAPK and GSK3beta. *Neurobiol. Dis.*, **44**, 142–151.
47. Kramer,O.H., Zhu,P., Ostendorff,H.P., Golebiewski,M., Tiefenbach,J., Peters,M.A., Brill,B., Groner,B., Bach,I., Heinzel,T. *et al.* (2003) The histone deacetylase inhibitor valproic acid selectively induces proteasomal degradation of HDAC2. *EMBO J.*, **22**, 3411–3420.